Why do they travel backwards? Understanding passenger travel behaviour in congested urban public transport systems

Yu, Chao; Li, Haiying; Wang, Ziyulong; Ma, Wei; Goverde, Rob M.P.; Cats, Oded

DOI
10.1016/j.tra.2025.104630

Publication date
2025

Document Version
Final published version

Published in
Transportation Research Part A: Policy and Practice

Transportation Research Part A xxx (xxxx) xxx

Contents lists available at ScienceDirect

Transportation Research Part A

journal homepage: www.elsevier.com/locate/tra

Why do they travel backwards? Understanding passenger travel behaviour in congested urban public transport systems

Chao Yu [a,b], Haiying Li [a], Ziyulong Wang [c], Wei Ma [b], Rob M.P. Goverde [c], Oded Cats [c,*]

[a] School of Traffic and Transportation, Beijing Jiaotong University, Beijing, 100044, China
[b] Department of Civil and Environmental Engineering, The Hong Kong Polytechnic University, 999077, Hong Kong, China
[c] Department of Transport and Planning, Delft University of Technology, Delft, 2628 CN, The Netherlands

ARTICLE INFO

Keywords:
Crowding
Travelling backwards
Metro systems
Revealed preference
Discrete choice model
Smart card data

ABSTRACT

Widespread congestion in metro systems often hinders passengers from boarding the first arriving train, making them compelled to adopt an alternative route, some of which involve travelling backwards. While this travel strategy has direct consequences for forecasting passenger flow distribution in congested networks, little is known about the travelling backwards phenomenon and why people adopt this travelling behaviour. The aim of this study is to understand passengers' perception of time in various segments considering travelling backwards. To achieve this, we develop a route choice model using revealed preference data from smart card records. We find that passengers exhibit a greater aversion to waiting time and onboard time while travelling backwards. Specifically, passengers perceive each minute spent waiting on the turn-back stations' platform as equivalent to 1.97 min on the origin platform. Similarly, each minute spent onboard the backwards train is perceived as equivalent to 1.24 min on the forwards train. Ignoring this difference in perception would result in the underestimation of the expected social benefits of demand management policies. Finally, we assess the potential benefits of travelling backwards under various passenger flow conditions, offering valuable policy insights regarding whether and how this behaviour should be regulated or promoted.

1. Introduction

Urbanisation spurs an agglomeration of population and economy, as well as leads to an overcrowded public transport (PT) system in many urban regions. This overcrowding induces discomfort and thereby leads to a longer perceived journey time (Pel et al., 2014; Yap et al., 2023). Studies have shown that dissatisfaction with crowding affects passengers' stress and overall health, thereby reducing their subjective well-being and even life satisfaction (Arbex and Cunha, 2020; Kumagai et al., 2021). As a result, coping with congestion in PT services becomes a daily challenge for urban residents in large cities, especially commuters (Haywood et al., 2017; Tirachini et al., 2017). Understanding passengers' route choice and their perceptions of overcrowding in urban PT systems is crucial for effective PT planning and operations. Accurately capturing these perceptions and route choices under overcrowded conditions is essential for formulating effective crowding alleviation strategies and improving PT passenger network assignment models (Yap and Cats, 2021).

* Corresponding author.
E-mail addresses: chao14.yu@polyu.edu.hk (C. Yu), hyli@bjtu.edu.cn (H. Li), z.wang-19@tudelft.nl (Z. Wang), wei.w.ma@polyu.edu.hk (W. Ma), r.m.p.goverde@tudelft.nl (R.M.P. Goverde), o.cats@tudelft.nl (O. Cats).

https://doi.org/10.1016/j.tra.2025.104630
Received 5 August 2024; Received in revised form 5 June 2025; Accepted 29 July 2025

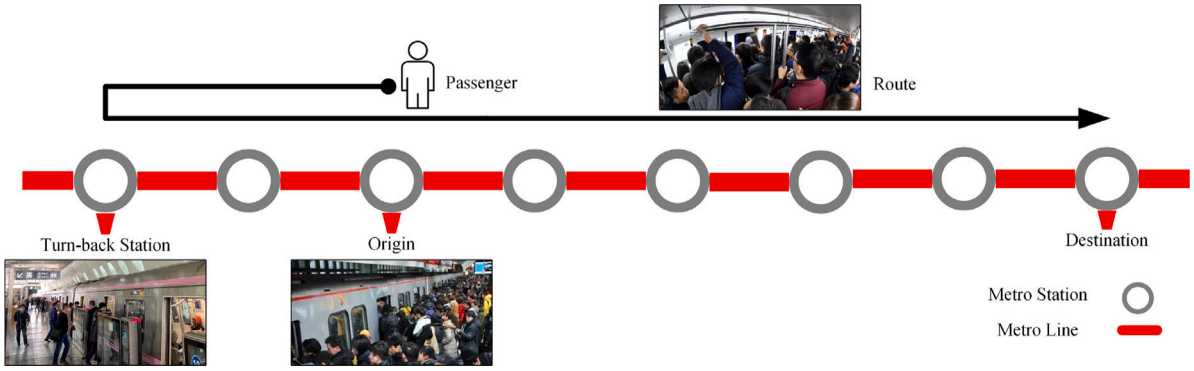

Fig. 1. Illustration of the passenger travelling backwards behaviour in congested urban public transport systems.

PT crowding may result in two distinctive impacts on the passenger travel experience in the event that the earliest arriving vehicle cannot be boarded. The first one is the prolonged waiting time experienced by passengers who are denied boarding when they are left behind waiting for the next arriving vehicle (Cats et al., 2016), which might occur multiple times during peak hours (Zhu et al., 2017). The second one involves responding to recurrent crowding conditions by adopting a strategy to minimise the risk of denied boarding as well as possibly increase the likelihood of obtaining a seat: they board a vehicle travelling in the opposite direction and then transfer at a turn-back station to continue in their original direction, as illustrated in Fig. 1. This "travelling backwards" phenomenon prevails at stations with high commuting traffic, where regular travellers are able to undertake such a behavioural adaptation based on past experience. A real-life scenario of passenger congestion, which often compels travellers to adopt the travelling backwards behaviour, is illustrated in Appendix A. Commuters frequently employ this strategy during peak hours to ensure punctual arrival at their workplaces since trains in the outbound direction usually experience lower levels of crowding than those in the inbound direction (Xu et al., 2018; Yu et al., 2020). Therefore, passengers travelling backwards can expect fewer instances of denied boarding and reduced time spent in crowded stations, hence alleviating frustration (Cats et al., 2016; Drabicki et al., 2023), improving the sense of safety (Björklund and Swärdh, 2017; Schneider et al., 2021) and decreasing the possibility of risk-taking behaviours (Zhou et al., 2023).

While the travel behaviour of left-behind passengers is by now relatively well-understood (Zhao et al., 2016; Zhu et al., 2018; Yap and Cats, 2021), comparable efforts to understand the travelling backwards behaviour are lacking, despite its increasing propensity in large and dense cities, such as Singapore, Beijing, and Hong Kong (Othman et al., 2015; Xu et al., 2018; Eltved, 2020). Traditional route choice models can hardly handle travelling backwards behaviour since routes containing loops are often excluded during the choice set generation phase (Raveau et al., 2011, 2014). Consequently, these models are unable to reproduce the travelling backwards behaviour and passenger flow estimates generated by these models are inaccurate, thereby hampering the development of effective passenger flow control and guidance strategies (Shi et al., 2022). There is therefore a growing need to develop methods to identify and understand this particular behaviour. Because such data are widely available and avoid the biases associated with stated preference methods, recent studies have used revealed preference data, such as those obtained from smart cards and train service timetables, to investigate this behaviour. The first attempt to examine the travelling backwards behaviour was made by Chakirov and Erath (2011) who utilised smart card data from Mass Rapid Transit in Singapore. They discovered that the waiting time distribution of commuters at one of the stations exhibited a bimodal distribution, in which the first peak corresponds to regular waiting times and the second peak indicates extra travel time due to travelling backwards. Further research by Li et al. (2017) and Xu et al. (2018) applied affinity propagation clustering and found that around 10% of passenger trips at some stations in Beijing involved travelling backwards. Yu et al. (2020) proposed a data-driven method based on Gaussian Mixture Models to model travelling backwards behaviour and utilised Bayesian theorem and a Markov Chain Monte Carlo algorithm to estimate model parameters. This method identified passengers travelling backwards with an error of about 5% when validated against observed ground truth data. In addition, Eltved (2020) investigated a related route choice behaviour, where passengers travel longer onboard to transfer at a less crowded station. This longer onboard travel behaviour was observed in the Mass Transit Railway of Hong Kong, with 35% to 55% of passengers during the evening peak opting for such a strategy. Notwithstanding, little is known about the considerations made by passengers who choose to travel backwards. Chakirov and Erath (2011) provided a rough estimation, suggesting that some passengers are willing to spend up to 10 min of additional travel time to secure a seat onboard. Building on the same case study of identified passengers with travelling backwards behaviour in Singapore, Tirachini et al. (2016) revealed the preference for securing a seat, partially elucidating the reason for travelling backwards. We hypothesise that the trade-off between travelling forwards and backwards involves multiple factors beyond seating preference, such as expected changes in travel time, platform congestion, onboard crowding and potential denied boarding. A research gap therefore exists in apprehending passengers' perceived travel time in each trip segment when travelling backwards, i.e., in understanding the trade-offs between the underlying determinants of this behaviour.

We address this knowledge gap by developing and applying a novel method to understand how passengers evaluate onboard and waiting times in relation to travelling backwards behaviour in crowded metro systems. Drawing on widely available revealed

preference data — principally smart card data — we capture passengers' perceptions with the explicit aim of informing policy-making and practical applications. Our approach involves reconstructing the travel trajectories of passengers, allowing us to segment waiting and onboard times into initial and additional components attributable to travelling backwards behaviour. This segmentation allows identifying the contributions of the additional waiting and onboard times associated with travelling backwards behaviour to passenger travel (dis)utilities. The estimated coefficients are then compared to each other and to those of other travel time components, such as denied boarding and initial waiting and onboard times. The inherent complexity of identifying and valuing travelling backwards behaviour, which often manifests itself in overcrowded situations at specific stations and within defined time bounds, poses significant empirical and modelling challenges. To tackle this complexity, we introduce an innovative choice set generation method tailored to individual travel records. It serves as the foundation for developing a discrete choice model using maximum likelihood estimation to estimate parameters that reflect passenger perceptions. Then, the proposed approach is applied to the Beijing metro network, examining how travelling backwards influences the effectiveness of demand management strategies. Additionally, we conduct experiments to assess the consequences of various proportions of passengers travelling backwards in different passenger flow scenarios. This analysis offers valuable policy implications regarding whether and how this behaviour should be regulated or promoted.

The remainder of this article is organised as follows: In Section 2, we describe the input data and propose the methodology for estimating route choice, generating the attributes, and modelling travelling backwards behaviour. Section 3 introduces the case study of the Beijing metro network, followed by the analysis of the results and a discussion of policy implications in Section 4. Finally, we conclude the paper in Section 5.

2. Methodology

In this section, we discuss the required data inputs (Section 2.1), model formulation (Section 2.2), and choice set generation procedure (Section 2.3).

2.1. Data input

The input data consists of smart card data, offline train timetable data, and survey data concerning walking time. The smart card data comprise travel records for individual passengers, with each record documenting the passenger's tap-in timestamp, tap-out timestamp, origin, and destination. As part of data pre-processing, travel records with a travel time exceeding 4 h are marked as abnormal and are removed from the dataset. We focus our analysis on single-route, no-transfer origin–destination (OD) pairs. This type of OD pair has only one feasible route, which does not involve transferring between different lines. This allows us to minimise the impact of multi-route choice and unstable transfer processes (involving additional walking time and waiting time) on the attribute estimation (Zhao et al., 2016; Yu et al., 2020). Eliminating these complexities allows us to understand better the core relationship under investigation, namely the trade-off between denied boarding and opting for travelling backwards. Moreover, it facilitates a more straightforward interpretation of the Revealed Preference data from the perspective of passenger perception, as it isolates the decision-making process to a single, continuous journey from origin to destination without the added complexity and uncertainty in journey inference which is induced by transfers (Yu et al., 2020). This focus is crucial because the benefits of travelling backwards at the origin station typically do not extend to subsequent legs of a journey involving transfers. For instance, a commuter may travel backwards to board a less crowded train, thus reducing waiting time. However, this benefit does not extend to subsequent legs if transfers are required, as passengers must again balance the trade-off between denied boarding and choosing to travel backwards at the transfer stations. The train timetable data consist of logs for each metro train, recording the arrival and departure timestamps at each station platform. The survey data provide the average access walking time and egress walking time for passengers at each station. Access walking time refers to the time it takes to walk from the tap-in gate to the platform, while egress walking time refers to the time taken to walk from the platform to the tap-out gate. For transfer stations with multiple platforms, the survey records the access and egress walking times for each platform separately.

2.2. Model formulation

In this section, we introduce the method for estimating the chosen route based on Revealed Preference data, and the methods for imputing attributes in the scenarios of denied boarding and travelling backwards, respectively. Based on the imputed attributes, passengers' perception of time in various segments is estimated using a utility-based discrete choice modelling framework.

2.2.1. Route choice estimation

We consider all route alternatives associated with either denied boarding or travelling backwards using a time-space representation. Herein, boarding a different train due to denied boarding or changing direction at a different turn-back station corresponds to distinctive alternative routes. Fig. 2 illustrates an example passenger journey including denied boarding and travelling backwards. In this case, five alternative routes are associated with denied boarding, and two additional routes are associated with travelling backwards. Note that even if the same train is boarded by following either travelling forwards or backwards behaviour (e.g., Train 4 in Fig. 2), these two options are treated as two alternative routes since the passenger journey components differ.

Based on the above-mentioned input data, we introduce the following notations in our model formulation: we define the metro system as a directed graph network $G = (S, E)$, where each node s ($s \in S$) represents a metro station and each edge e ($e \in E$)

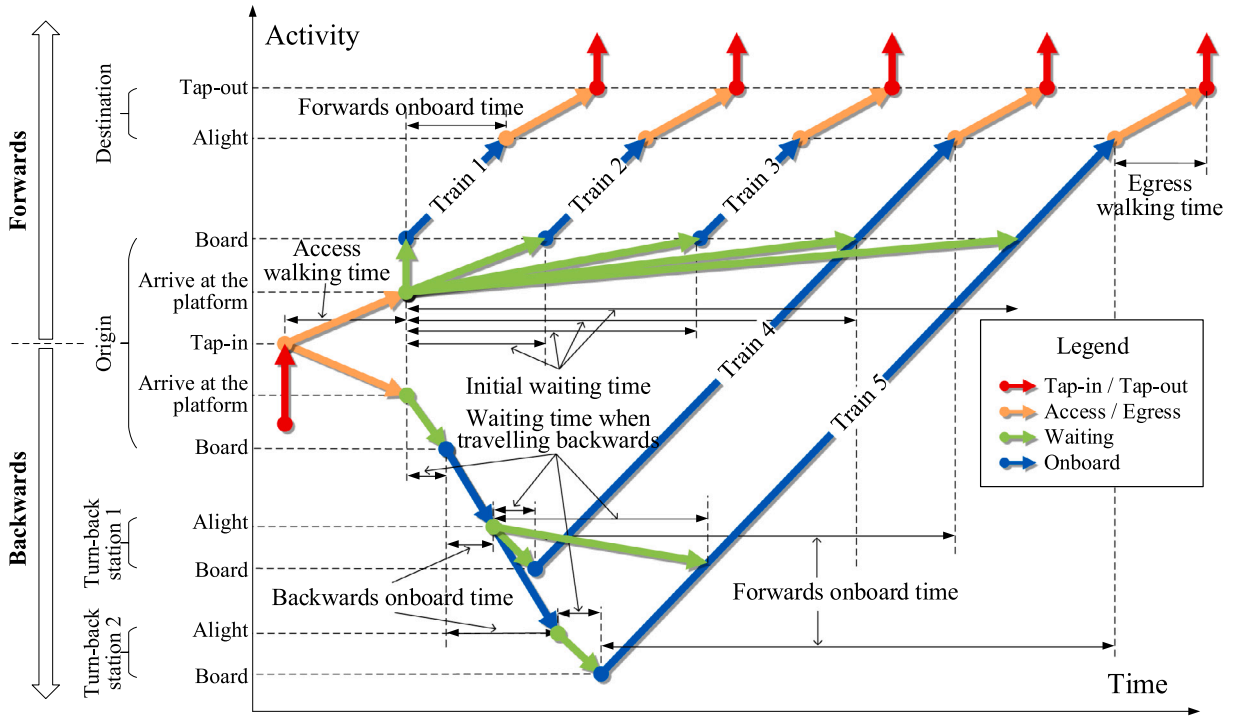

Fig. 2. An example of a passenger journey that comprises denied boarding and travelling backwards.

represents a metro service section between two stations. For each passenger i, we define the tap-in timestamp as t_i^+ and the tap-out timestamp as t_i^-. The origin and destination are denoted as o_i and d_i, respectively. The set of all ordered trains is represented by H, where $H = \{h_1, h_2, \ldots, h_n\}$, and n denotes the total number of trains. For each train h_k in H, $t_{h_k}^{s,a}$ is the arrival timestamp of train h_k at station s, and $t_{h_k}^{s,d}$ the departure timestamp from station s. Additionally, we define the access walking time to station s as t_s^+ and the egress walking time as t_s^-, respectively. Finally, the platform area of station s is of size a_s.

Given a passenger i, the utility of each alternative route is calculated using walking time t_i^{wkt}, waiting time t_i^{wtt}, onboard time t_i^{obt}, platform passenger density d_i, and train load factor l_i as explanatory variables. Further, as shown in Fig. 2, we distinguish between the initial waiting time $t_i^{wtt,in}$ and waiting time when travelling backwards $t_i^{wtt,tb}$, and between forwards onboard time $t_i^{obt,f}$ and backwards onboard time $t_i^{obt,b}$. To infer the values of the above explanatory variables, it is first necessary to determine whether a given passenger adopts the denied boarding strategy or the travelling backwards strategy based on the travel time. Given a passenger i, the travel time tt_i can be calculated as follows.

$$tt_i = t_i^- - t_i^+ \tag{1}$$

We utilise the Gaussian mixture model-based method developed by Yu et al. (2020) to estimate the probability of choosing each alternative route, considering travelling backwards for a given travel time in each time slot. Given that this method was found to yield an error of less than 5%, we adopt this method in this study. The following example illustrates how to use the above-estimated probability to assist in classifying denied boarding and travelling backwards. Assume that within a time slot, there are N passengers with travel times ranging from t_m to $(t_m+\Delta t)$ seconds. The probabilities of them choosing the denied boarding and travelling backwards are calibrated as p and $(1-p)$ respectively. Hence, we identify $N\cdot p$ passengers as adopting denied boarding, and the remaining $N\cdot(1-p)$ passengers are considered to travel backwards. Admittedly, the above probability-to-frequency conversion may result in false positives or false negatives — i.e., an individual who adopts denied boarding is mistakenly assigned to travelling backwards, or an individual who adopts travelling backwards is mistakenly assigned to denied boarding — assignments at the individual record level. This potential misalignment at the individual level is, however, arguably negligible in understanding travelling backwards behaviour for the following two reasons. First, the average platform passenger density and train load factor that need to be calculated in the subsequent step, detailed in the next section, are only related to the passenger flow allocated to each alternative route and are not affected by the reconstructed routes of individual passengers. Second, subsequent discrete choice models are calibrated by minimising the log-likelihood function, incorporating the utility of each journey record into the log-likelihood function. Consequently, potential individual-level error does not affect the parameter estimation results obtained by our analysis (Ma and Qian, 2017). Based on the identified strategy (denied boarding or travelling backwards), the following steps are undertaken in order to obtain the relevant attribute values.

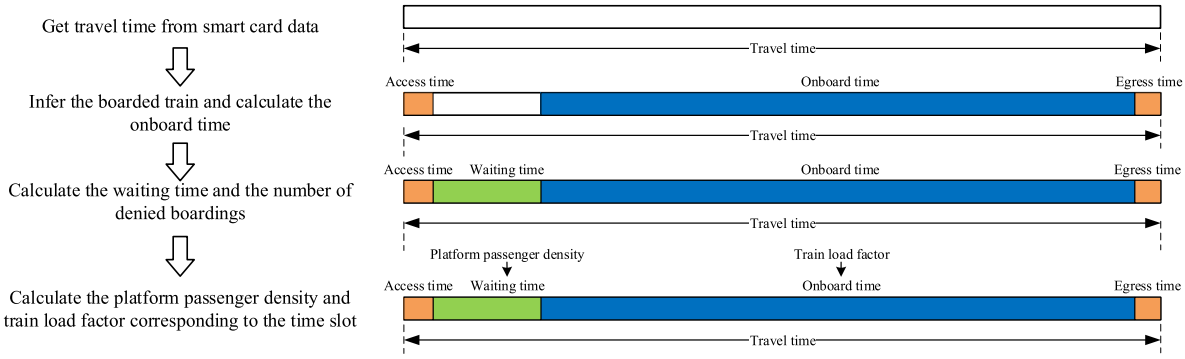

Fig. 3. Attribute imputation when denied boarding.

2.2.2. Obtaining attribute values for denied boarding

Fig. 3 shows the process of attribute imputation when passengers experience denied boarding. For a given passenger i, the timestamp $\omega^i_{o_i}$ of arrival at the platform of station o_i is:

$$\omega^i_{o_i} = t^+_i + t^+_{o_i} \tag{2}$$

The timestamp $\tau^i_{d_i}$ of arrival at the platform of station d_i can be calculated using:

$$\tau^i_{d_i} = t^-_i - t^-_{d_i} \tag{3}$$

The train $\tilde{h}_i$ that passenger i has most likely boarded can be determined by Eq. (4) which returns the train that minimises the time difference, subject to the constraint that the train arrives before or exactly at $\tau^i_{d_i}$.

$$\tilde{h}_i = \underset{h_k \in H : t^{d_i,a}_{h_k} \le \tau^i_{d_i}}{\operatorname{argmin}} (\tau^i_{d_i} - t^{d_i,a}_{h_k}) \tag{4}$$

According to the timestamp $\omega^i_{o_i}$ of arrival at the platform and the departure timestamp of the train $\tilde{h}_i$ at station o_i, the initial waiting time $t^{wtt,in}_i$ of passenger i at station o_i is:

$$t^{wtt,in}_i = t^{o_i,d}_{\tilde{h}_i} - \omega^i_{o_i} \tag{5}$$

The forwards onboard time $t^{obt,f}_i$ can be calculated as:

$$t^{obt,f}_i = t^{d_i,a}_{\tilde{h}_i} - t^{o_i,d}_{\tilde{h}_i} \tag{6}$$

The walking time t^{wkt}_i can be calculated as:

$$t^{wkt}_i = t^+_{o_i} + t^-_{d_i} \tag{7}$$

Given that the above travel process does not involve travelling backwards, the waiting time when travelling backwards $t^{wtt,tb}_i$ and backwards onboard time $t^{obt,b}_i$ are set to null.

$$t^{wtt,tb}_i = 0,\ t^{obt,b}_i = 0 \tag{8}$$

2.2.3. Obtaining attribute values for travelling backwards

The process of attribute imputation when travelling backwards is shown in Fig. 4. The timestamp of arrival at the platform $\omega^i_{o_i}$ of station o_i and timestamp of arrival at the platform $\tau^i_{d_i}$ of station d_i of passenger i are calculated according to Eqs. (2) and (3). The walking time t^{wkt}_i can be calculated by Eq. (7). Unlike denied boarding, the departure station of the last trip for passengers who adopt the travelling backwards strategy is the turn-back station rather than the origin. The selected specific turn-back station, s_{tb}, can be determined based on the travel time and headway (see Yu et al. (2020) for more details). The backwards train $\tilde{h}_{i,tb}$ that passenger i is most likely to have taken can be determined according to Eq. (9), where H_{tb} corresponds to the set of all ordered trains in the backwards direction of passenger travel. This formula assumes that passengers will not encounter denied boarding in the backwards direction, which is reasonable because several studies have shown that trains used for travelling backwards are less crowded (Tirachini et al., 2016; Xu et al., 2018; Yu et al., 2020).

$$\tilde{h}_{i,tb} = \underset{h_k \in H_{tb} : \omega^i_{o_i} \le t^{o_i,d}_{h_k}}{\operatorname{argmin}} (t^{o_i,d}_{h_k} - \omega^i_{o_i}) \tag{9}$$

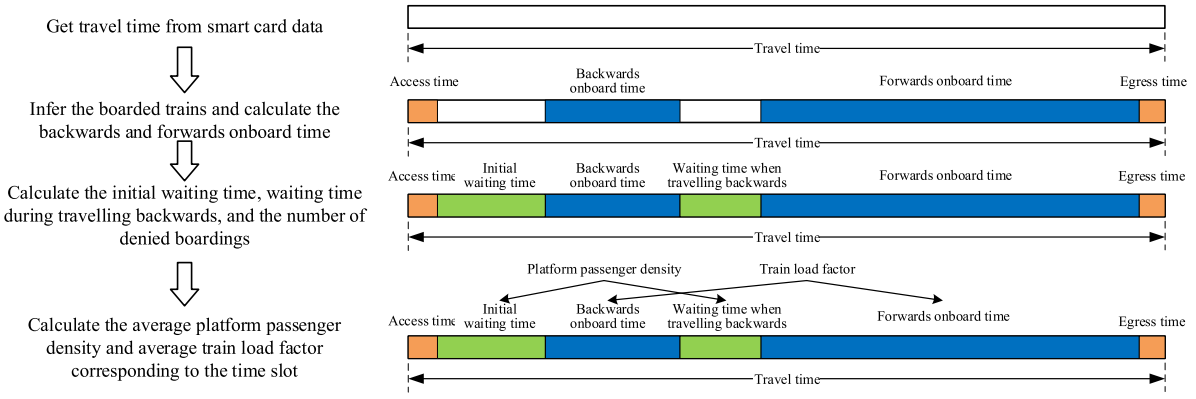

Fig. 4. Attribute imputation when travelling backwards.

The forwards train $\tilde{h}_{i,f}$ that passenger i is most likely to have taken can be determined using:

$$\tilde{h}_{i,f} = \underset{h_k \in H : t_{h_k}^{d_i,a} \le \tau_{d_i}^i}{\operatorname{argmin}} \left(\tau_{d_i}^i - t_{h_k}^{d_i,a}\right) \tag{10}$$

According to the determined backwards train $\tilde{h}_{i,tb}$ and forwards train $\tilde{h}_{i,f}$, the initial waiting time $t_i^{wtt,in}$ of passenger i at origin o_i can be calculated as Eq. (11).

$$t_i^{wtt,in} = t_{\tilde{h}_{i,tb}}^{o_i,d} - \omega_{o_i}^i \tag{11}$$

The waiting time when travelling backwards $t_i^{wtt,tb}$ of passenger i at turn back station s_{tb} can be calculated as Eq. (12).

$$t_i^{wtt,tb} = t_{\tilde{h}_{i,f}}^{s_{tb},d} - t_{\tilde{h}_{i,tb}}^{s_{tb},a} \tag{12}$$

The backwards onboard time $t_i^{obt,b}$ of passenger i is calculated as follows:

$$t_i^{obt,b} = t_{\tilde{h}_{i,tb}}^{s_{tb},a} - t_{\tilde{h}_{i,tb}}^{o_i,d} \tag{13}$$

The forwards onboard time $t_i^{obt,f}$ of passenger i is calculated as follows:

$$t_i^{obt,f} = t_{\tilde{h}_{i,f}}^{d_i,a} - t_{\tilde{h}_{i,f}}^{s_{tb},d} \tag{14}$$

2.2.4. Attribute imputation for platform passenger density and train load factor

The attribute imputation processes for denied boarding and travelling backwards reconstruct passengers' trajectories. By superimposing those, one can obtain estimates of passenger loads throughout the network. Consequently, the platform passenger density and train load factor can be calculated based on these passenger load distribution results. The average platform passenger density $\bar{D}_{o_i}^i$ experienced by passenger i who is denied boarding at the origin station can be calculated using Eq. (15), where $N_{o_i}(t)$ is the number of passengers at platform o_i at time t. This integral function can be approximated by numerical methods, such as averaging the density of each minute from $\omega_{o_i}^i$ to $t_{\tilde{h}_i}^{o_i,d}$ (Hänseler et al., 2020a).

$$\bar{D}_{o_i}^i = \frac{1}{t_i^{wtt,in}} \int_{\omega_{o_i}^i}^{t_{\tilde{h}_i}^{o_i,d}} \frac{N_{o_i}(t)}{a_{o_i}} dt \tag{15}$$

Further, the average platform passenger density $\bar{D}_{o_i,tb}^i$ experienced by passenger i who adopts the travelling backwards strategy at station o_i and $\bar{D}_{s_{tb},f}^i$ of the forward strategy at station s_{tb} can be calculated by Eq. (16).

$$\bar{D}_{o_i,tb}^i = \frac{1}{t_i^{wtt,in}} \int_{\omega_{o_i}^i}^{t_{\tilde{h}_{i,tb}}^{o_i,d}} \frac{N_{o_i}(t)}{a_{o_i}} dt, \quad \bar{D}_{s_{tb},f}^i = \frac{1}{t_i^{wtt,tb}} \int_{t_{\tilde{h}_{i,tb}}^{s_{tb},a}}^{t_{\tilde{h}_{i,f}}^{s_{tb},d}} \frac{N_{s_{tb}}(t)}{a_{s_{tb}}} dt \tag{16}$$

The average train load factor $\bar{l}_i$ experienced by passenger i who is denied boarding can be calculated according to Eq. (17), where E_i corresponds to the set of all sections passed by passenger i, $n(E_i)$ is the number of sections passed, $C_{e_i}(\tilde{h}_i)$ is the number of passengers of train $\tilde{h}_i$ in section e_i, and $C^{\max}(\tilde{h}_i)$ is the maximum capacity of train $\tilde{h}_i$.

$$\bar{l}_i = \frac{1}{n(E_i)} \sum_{e_i \in E_i} \frac{C_{e_i}(\tilde{h}_i)}{C^{\max}(\tilde{h}_i)} \tag{17}$$

The average train load factor $\bar{l}_{i,tb}$ in the backwards direction and $\bar{l}_{i,f}$ in the forwards direction experienced by passenger i who adopts a travelling backwards strategy can be calculated according to Eq. (18), where $E_{i,tb}$ and $E_{i,f}$ corresponds to the set of all sections in backwards and forwards direction passed by passenger i.

$$\bar{l}_{i,tb} = \frac{1}{n(E_{i,tb})} \sum_{e_i \in E_{i,tb}} \frac{C_{e_i}(\tilde{h}_{i,tb})}{C^{\max}(\tilde{h}_{i,tb})}, \ \bar{l}_{i,f} = \frac{1}{n(E_{i,f})} \sum_{e_i \in E_{i,f}} \frac{C_{e_i}(\tilde{h}_{i,f})}{C^{\max}(\tilde{h}_{i,f})} \tag{18}$$

Note that passengers perceive discomfort only when crowding levels exceed a certain threshold. This relation is empirically underpinned by various studies on the expected travel comfort of passengers (Kim et al., 2020; Yap et al., 2023; Zhou et al., 2023). Since travelling backwards behaviour typically occurs in overcrowding scenarios, it is necessary to quantify the threshold at which discomfort becomes noticeable. At this point, we define the critical platform passenger density for discomfort as d_m, and the critical train load factor as l_m.

For passenger i who is denied boarding, platform passenger density d_i is calculated as:

$$d_i = \max\left(\bar{D}^i_{o_i} - d_m, 0\right) \tag{19}$$

The train load factor l_i is calculated as:

$$l_i = \max\left(\bar{l}_i - l_m, 0\right) \tag{20}$$

For passenger i who adopts the travelling backwards strategy, we calculate the adjusted average platform passenger density based on the passenger's travel time in each segment. The corresponding variable d_i can be calculated by:

$$d_i = \max\left(\frac{\left(\bar{D}^i_{o_i,tb} - d_m\right) \cdot t_i^{wtt,in} + \left(\bar{D}^i_{s_{tb},f} - d_m\right) \cdot t_i^{wtt,tb}}{t_i^{wtt,in} + t_i^{wtt,in}}, 0\right) \tag{21}$$

Similarly, we calculate the adjusted average train load factor based on the number of passed sections. The corresponding variable l_i can be calculated as:

$$l_i = \max\left(\frac{\left(\bar{l}_{i,tb} - l_m\right) \cdot n(E_{i,tb}) + \left(\bar{l}_{i,f} - l_m\right) \cdot n(E_{i,f})}{n(E_{i,tb}) + n(E_{i,f})}, 0\right) \tag{22}$$

2.2.5. Route choice model estimation

Based on all the obtained attribute values, we estimate a discrete choice model where the set of all routes is R and each route with travelling backwards behaviour is denoted as $r \in R_b$, where R_b is a route set with backwards travelling behaviour, $R_b \subset R$. Given passenger i choosing route r, the utility U_i^r consists of a deterministic utility V_i^r, which is a function of various explanatory variables and a random utility term ϵ_i^r, which is given as:

$$U_i^r = V_i^r + \epsilon_i^r \tag{23}$$

To capture the complex relationship between explanatory variables and passenger choice, a Mixed Logit model is estimated in order to account for the panel nature of the data, i.e., the dataset includes multiple observations associated with the same cardholder. to calculate the deterministic utility. This model combines platform passenger density with waiting time and load factor with onboard time. The deterministic utility of any given route can be calculated as follows:

$$V_i^r = \beta^{wkt} \cdot t_i^{wkt} + (\beta^{wtt,in} \cdot t_i^{wtt,in} + \beta^{wtt,tb} \cdot t_i^{wtt,tb}) \cdot (1 + \beta^d \cdot d_i) + (\beta^{obt,f} \cdot t_i^{obt,f} + \beta^{obt,b} \cdot t_i^{obt,b}) \cdot (1 + \beta^l \cdot l_i) \tag{24}$$

The explanatory variables included in Eq. (24) are specified based on the attribute imputation process described above. The coefficients β are estimated using PythonBiogeme, which iteratively seeks to minimise the log-likelihood function. The Newton algorithm with simple bounds is used as an optimisation algorithm, estimating the parameters iteratively (Myung, 2003).

The above Mixed Logit model assumes that the alternatives are mutually independent, lacking any nested structures or correlations. However, in this study, passengers' route choices may not necessarily be strictly independent; rather, they involve two distinct categories, namely denied boarding and travelling backwards. Consequently, it is necessary to calibrate a choice model that incorporates a nested structure to explore the correlations between alternatives within each category. To construct a Nested Logit model, the alternative route r is assigned to two nests numbered by w, $r \in R_w$, $w \in W$, where W represents the set of nests containing denied boarding and travelling backwards, and R_w represents all alternative routes within the nest w. Here, the probability of route r being chosen can be calculated as:

$$P(r, w) = P(r \mid w) \cdot P(w), \quad r \in R_w, \ w \in W \tag{25}$$

The probability of the nest w being chosen can be calculated by Eq. (26), where μ is a scale parameter associated with the choice between different nests, and $V^*_{i,w}$ represents the expected value of the utility of all alternative routes in the nest w.

$$P(w) = \frac{\exp(\mu \cdot V^*_{i,w})}{\sum_{w \in W} \exp(\mu \cdot V^*_{i,w})} \tag{26}$$

For a given nest w, $V^*_{i,w}$ can be computed using Eq. (27), where μ_w is the scale parameter associated with the choice between the alternative routes within the nest w, the V_i^r can be calculated using Eq. (24).

$$V^*_{i,w} = \frac{1}{\mu_w} \ln\left(\sum_{r \in R_w} \exp(\mu_w \cdot V_i^r)\right) \tag{27}$$

The conditional probability $P(r \mid w)$ can be calculated by Eq. (28).

$$P(r \mid w) = \frac{\exp(\mu_w \cdot V_i^r)}{\sum_{r \in R_w} \exp(\mu_w \cdot V_i^r)} \tag{28}$$

The parameter μ is typically normalised to 1, and μ_w needs to be calibrated to reflect the intrinsic relationship between the different choices within the nest. The parameters in the Nested Logit model are estimated using the Newton algorithm in PythonBiogeme (Bierlaire, 2016).

The robustness and significance of the estimated parameters are ascertained using robust t-tests and robust p-values for all the aforementioned Logit-based models with varying nesting structures. The goodness-of-fit of the models is evaluated using the Akaike Information Criterion (AIC), Bayesian Information Criterion (BIC), Rho-square, and Rho-square-bar statistics.

2.3. Choice-set generation process

Compared to conventional route choice contexts, incorporating travelling backwards adds additional constraints to the generation of the choice set, as mentioned in Section 1. To effectively capture the trade-offs experienced by passengers when choosing between passive denied boarding at the platform and actively adopting the travelling backwards strategy, a customised choice set generation method is designed below.

First, for each specific travel time, a corresponding choice set is constructed. Given a travel time, passengers with that travel time are inferred to choose specific routes according to the methods described in Sections 2.2.2 and 2.2.3. These inferred routes are then included in the choice set corresponding to that travel time. This approach helps reduce the interference of infeasible alternatives on model calibration.

Second, we filter the data to include only those passengers who have a potential reason to consider travelling backwards alternatives and therefore have both denied boarding alternatives and travelling backwards alternatives in their choice set. For instance, passengers whose travel times are shorter than the theoretical minimum time required for travelling backwards are excluded from the analysis, as these passengers cannot be used to capture their trade-off between denied boarding and travelling backwards.

Furthermore, when calibrating models with a nested structure, it is necessary to screen for records that have more than one alternative within each nest. Unlike models without a nested structure, the formulations in Nested Logit model shown as Eq. (26) and (28) contain parameters that reflect the correlation of choices within and across nests, requiring records with multiple intra-nest alternatives for calibration.

3. Case study

We apply the proposed method to the Changping Line in the Beijing metro network to estimate passengers' route choice and related trade-offs between various travel time components considering travelling backwards behaviour. As displayed in Fig. 5, the Changping Line is located in the northwest corner of Beijing, serving as a commuting route for residents of the Changping suburban areas to the central parts of the city. The case study utilises smart card data and train timetable data from all weekday morning peak hours, 7–9 AM, in September 2018. The average headway of train services on this line is 6.07 min on weekdays and 9.08 min on weekends. In particular, the average headway is even shortened to 4.14 min during weekday morning peak period to meet the high travel demand.

Despite this, commuters still face overcrowding on a daily basis, leading to frequent occurrences of travelling backwards behaviour amongst passengers who have their origin at Shahe and Shahe Gaojiaoyuan stations. These passengers' destinations are typically stations in the central urban area, such as Xierqi station, and they often travel backwards to Nanshao or Beishaowa stations before heading towards their intended destinations. The results of our analysis suggest that on average of 21% of passengers departing from Shahe travel backwards during morning rush hours, while the corresponding figure for passengers originating from Shahe Gaojiaoyuan is 9%.

The identification results have been validated against survey data collected in collaboration with the Beijing Metro Network Control Centre, with errors consistently under the 5% level (Yu et al., 2020). To obtain ground-truth observations of backwards travel, investigators boarded trains in the opposite direction and recorded the number of passengers who alighted at each turn-back station, crossed to the opposite platform, and waited to reboard a train continuing in their original direction. Each investigator was responsible for one carriage, and counting was conducted during the train's dwell time at the station, typically around 40 s, which provided sufficient time for conducting these observations. Passengers showing this behaviour were identified as engaging in backwards travel. A schematic diagram of the survey procedure is presented in Fig. 6. The aggregated survey counts were then

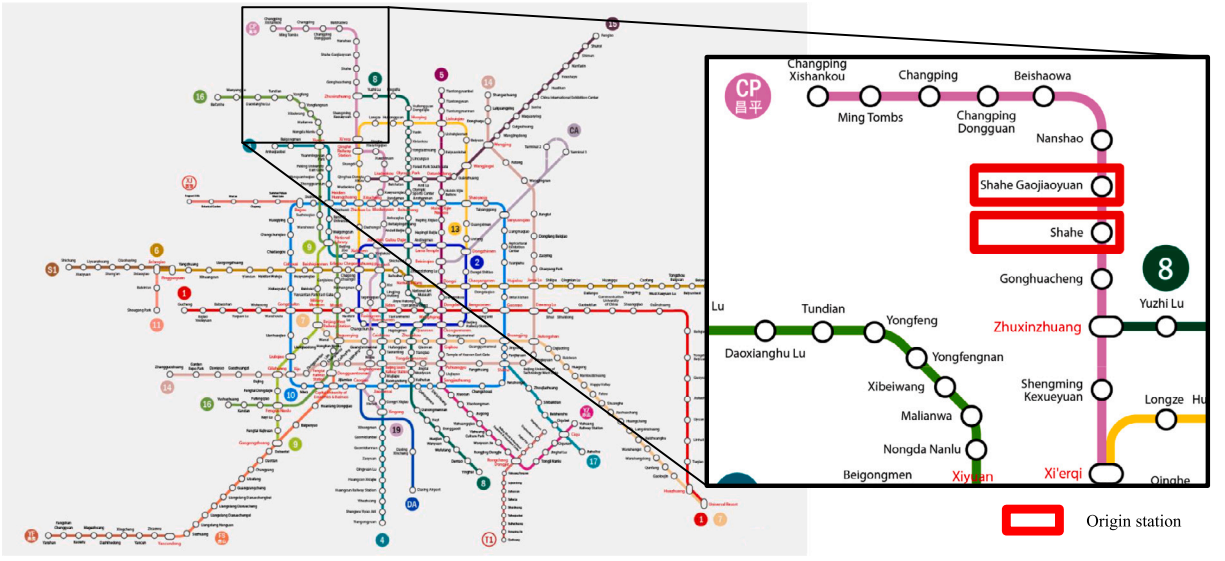

Fig. 5. Location of the case study stations in the Beijing metro network.

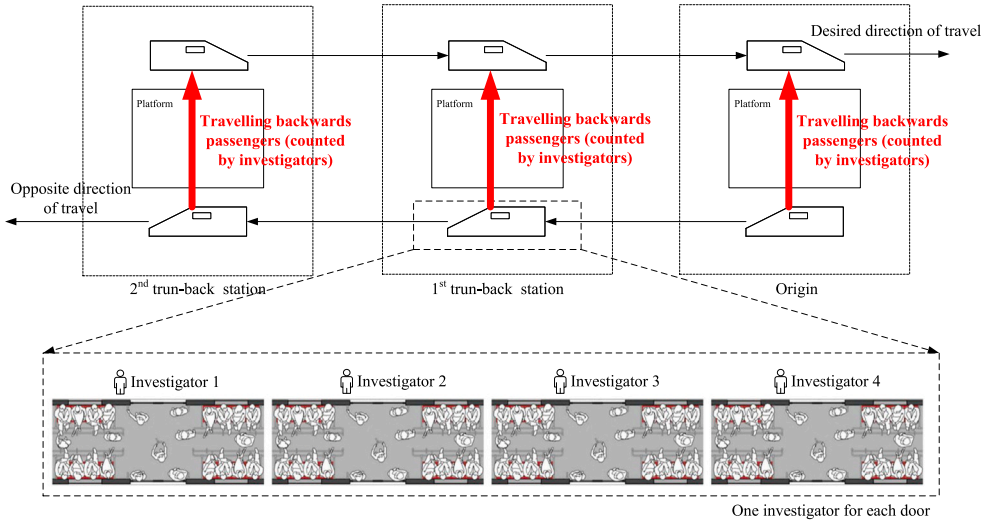

Fig. 6. Schematic overview of the field survey procedure used to identify passengers engaging in backwards travel at turn-back stations.

compared with the model-inferred results, confirming a close alignment and thereby demonstrating the robustness of the inference method.

Specifically, Fig. 7 presents the share of passengers exhibiting a travelling backwards behaviour for trips originating from these two stations, aggregated in 15 min intervals during the morning peak, reaching as high as 45% at Shahe and 23% at Shahe Gaojiaoyuan. A total of 63,804 trips originating from these two stations and terminating in the central area were recorded. After filtering out records with travel times shorter than the theoretical minimum time required for travelling backwards, 46,848 records remained available for calibrating the Mixed Logit model. Furthermore, by excluding those records with only one alternative within the nest, as described in Section 2.3, 17,802 records were obtained for calibrating the Nested Logit model. The estimation results are shown in Section 4.1.

4. Results

In this section, we first present the passenger flow assignment considering travelling backwards and estimation results of the route choice model in Section 4.1 and then apply our model to manage demands and guide passenger behaviours in Section 4.2.

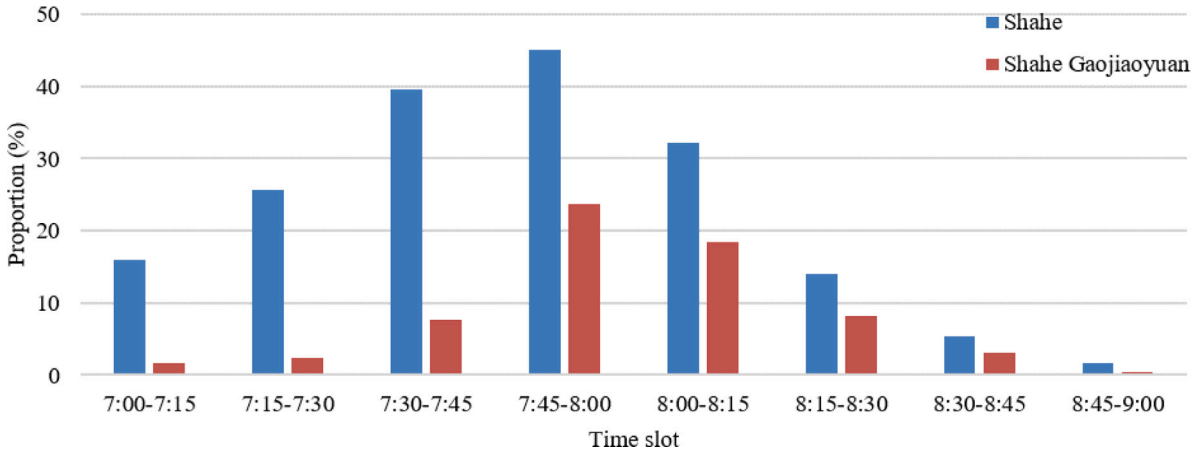

Fig. 7. Distribution of passengers who travel backwards during the morning peak period.

4.1. Model estimation results

In this subsection, we first demonstrate how the results of the analysis, which considers travelling backwards behaviour, improve the existing evaluation of passenger flow distribution. Subsequently, we present the evaluation metrics of the different models to identify the model form that best describes the behaviour of travelling backwards. Finally, the weights and physical meanings corresponding to each parameter in the best-performing model are analysed.

4.1.1. Passenger flow assignment considering travelling backwards

Based on the methods described in Sections 2.2.2 and 2.2.3, we can infer the train that each passenger boards, which is a crucial input for passenger flow assignment. Given a train timetable, in the absence of considering travelling backwards, the train chosen by a passenger can be calculated using Eq. (4). However, when considering travelling backwards, Eqs. (9) and (10) are additionally employed to determine the train selected by passengers who adopt the travelling backwards strategy. The decision to adopt the travelling backwards strategy is determined according to the method described in Section 2.2.1. Taking the morning peak on 26 September 2018 as an example, we present the load factors of the trains running in the direction from Changping suburban areas to central areas during the study period, as shown in Fig. 8. It can be observed that when travelling backwards is not considered, trains No. 1030, No. 1035, No. 1037, and No. 1038 are calculated to have load factors exceeding 130% in the Shahe-Gonghuacheng and Gonghuacheng-Zhuxinzhuang sections, with the highest reaching 165%. In the Beijing metro, a load factor of 100% implies 6 standing passengers per square metre (Chen et al., 2016). A load factor of 165% would suggest 9.9 standing passengers per square metre, which evidently exceeds the physical limit, i.e., resulting in an unrealistically over-estimated crowding level. In contrast, when travelling backwards is considered, the passenger flow assignment results are more reasonable, with the highest load factor being 120%. This indicates that considering travelling backwards can more realistically reflect the actual situation and provide a more accurate basis for calibrating passengers' perceptions in such overcrowded conditions.

4.1.2. Model estimation summary

A comparison of the different discrete choice models is summarised in Table 1. All of these models reach convergence within a computational time of 4.86 s on a PC with 16 GB RAM and an Intel I7 core processor. It is important to note that the values of d_m and l_m influence the calibration results of the models. The results presented here are the best-performing ones for each model, obtained after testing all possible combinations of d_m and l_m. The Nested Logit model exhibits higher Rho-square-bar values compared to the Mixed Logit model, indicating that passengers' choices have a clear hierarchical structure when considering the scenario of travelling backwards (Bierlaire, 2016). Further comparison between these two models shows that the Nested Logit model demonstrates the highest Rho-square-bar value of 0.247, the smallest AIC value of 18,228, and the BIC value of 18,290. Given the superior goodness-of-fit of the Nested Logit model, we employ the parameter estimation results from this model to analyse the travelling backwards behaviour in Section 4.1.3.

4.1.3. Parameter estimation results

As part of our model formulation, there are two variables with a threshold value for passengers' perception: platform density and load factor. Therefore, the impact of different critical platform density d_m and critical load factor l_m settings on model performance is first evaluated in order to select the most reasonable and best-performing values. Fig. 9 shows the empirical distributions of platform passenger density and load factor during the study period. We observe that the platform passenger density is mainly concentrated between 3.5 and 4.5 passengers per square metre, while the load factor is concentrated between 1.0 and 1.3.

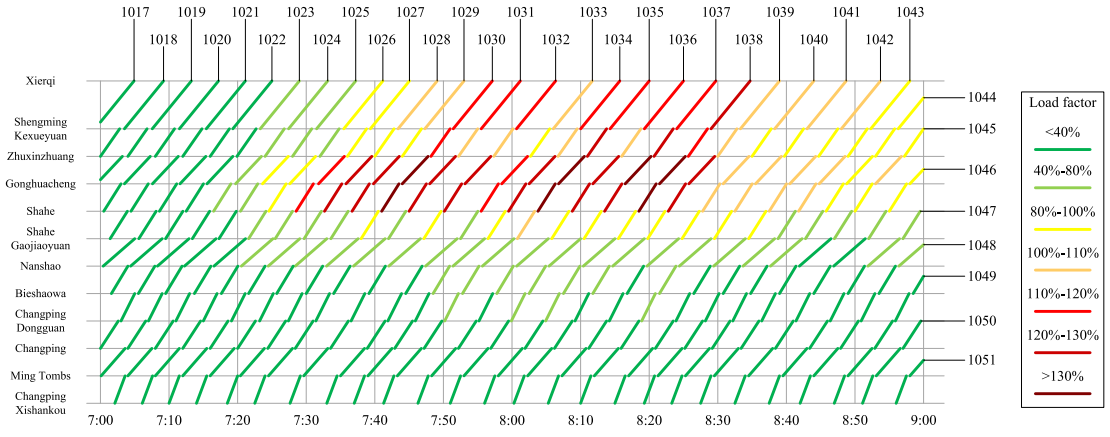

Passenger flow distribution without considering travelling backwards

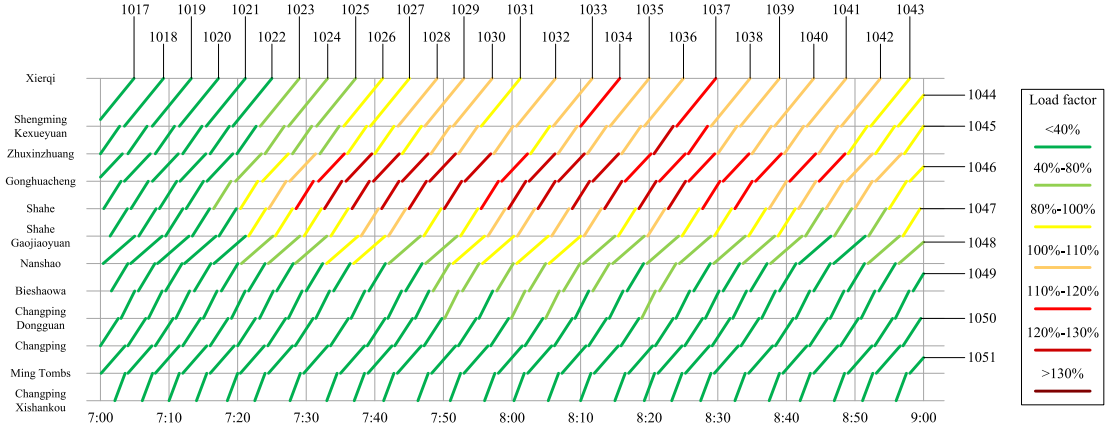

Passenger flow distribution considering travelling backwards

Fig. 8. Passenger flow distributions with and without considering travelling backwards.

Table 1
Model estimation summary.

Model	Mixed Logit model	Nested Logit model
Observations	46,848	17,802
Number of parameters	6	8
Initial log-likelihood	−32,474	−12,105
Final log-likelihood	−25,282	−9,106
Rho-square	0.221	0.248
Rho-square-bar	0.221	0.247
AIC	50,576	18,228
BIC	50,628	18,290

As a result, experiments are conducted using d_m values of [2.0, 2.5, 3.0, 3.5, 4.0, 4.5, 5.0, 5.5] and l_m values of [0.5, 0.6, 0.7, 0.8, 0.9, 1.0, 1.1, 1.2, 1.3]. The log-likelihood results in the Nested Logit model are shown in Fig. 10. When both d_m and l_m are large, variables d and l are found to be insignificant in the estimation results, hence the log-likelihoods are not shown in Fig. 10. This is reasonable since large d_m or l_m variables related to platform passenger density and load factor are processed as zero, making it difficult for these samples to provide effective perception information. The model performs best, i.e., yielding the smallest log-likelihood values of −9,106, with $d_m = 3.0$ and $l_m = 0.8$.

The above results imply that passengers begin to feel uncomfortable when platform density reaches 3 passengers per square metre, resulting in negative perceived utilities. This finding is consistent with the results of studies on platform density evaluation. For example, Nelson (2002) found that serious congestion is likely to occur if platform density exceeds 3.8 passengers per square metre. Similarly, a risk analysis report based on Shenzhen metro platforms states that a crowding degree of more than 3 passengers per square metre can be defined as a high-risk level (Zhou et al., 2023). This indicates that passengers may gradually feel uncomfortable

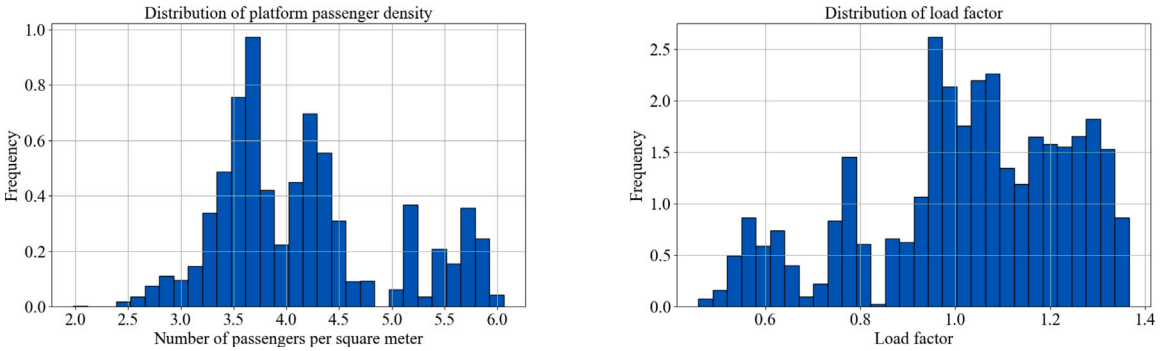

Fig. 9. Empirical distributions of platform passenger density and load factor.

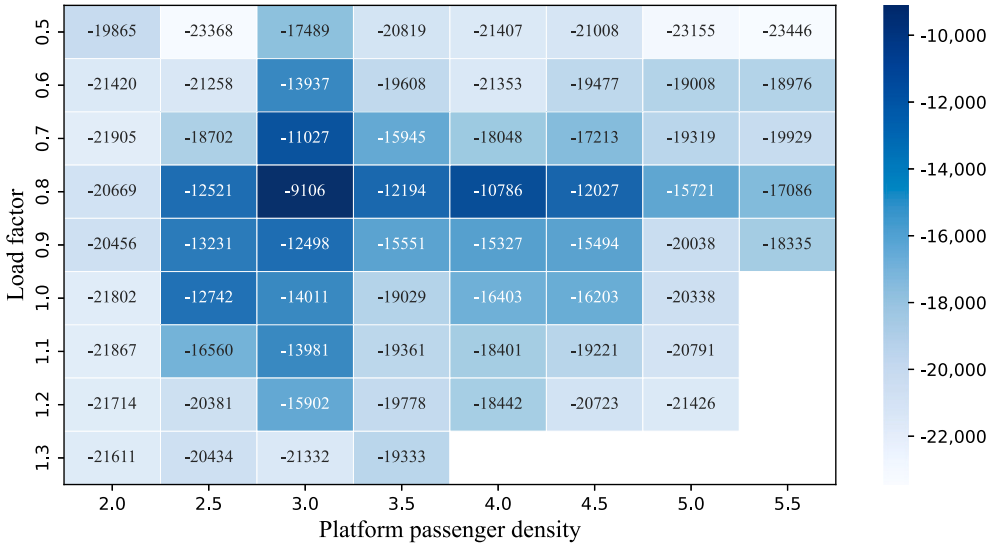

Fig. 10. Log likelihood values with various platform passenger density and load factor.

or even potentially endangered when the density exceeds this threshold. Moreover, the load factor threshold at which passengers begin to perceive disutility is 0.8. Note that while some past studies (Yap and Cats, 2021; Yap et al., 2023) defined the load factor as the ratio of the number of passengers to the seating capacity, we employ a different definition better suited for our case study. In Beijing, metro vehicles have only a limited number of seats to maximise supply capacity with most areas designed for standing. We adopt the definition used by Beijing metro design specifications, where a load factor of 1 corresponds to 6 passengers per square metre (Chen et al., 2016).

With $d_m = 3.0$ and $l_m = 0.8$, the estimated parameters for the Nested Logit model are reported in Table 2. The variable walking time t^{wkt} is found to be statistically insignificant due to the minimal difference in walking time across different observations. The remaining eight variables are all statistically significant with robust p-values smaller than 0.05.

Regarding the scale parameters associated with the nested structure, the upper-level scale parameter μ is normalised to 1. The estimated values of μ/μ_{db} and μ/μ_{tb} are 0.994 and 0.574, respectively. The ratio of scale parameters reflects the correlation among the alternatives within each nest. The value of μ/μ_{db}, being close to 1, indicates a low correlation among the alternatives within the nest involving denied boarding behaviour. This implies that passengers are more independent in choosing different trains upon denied boarding. Conversely, the value of μ/μ_{tb}, being considerably less than 1, suggests a high correlation among the alternatives within the nest involving travelling backwards behaviour. This indicates that passengers are more likely to be influenced by other alternatives when choosing a turn-back station. Furthermore, the scale parameter μ_{tb} is significantly smaller than μ, indicating a low correlation between the decision process involving travelling backwards and the upper-level decision process. This implies that passengers emphasise the specific factors of different turn-back stations, such as their platform passenger densities, when making decisions related to travelling backwards.

The estimated results for passengers' perception of time related to platform passenger density and load factor ($\beta^d = -0.655$ and $\beta^l = -0.964$) are illustrated in Fig. 11 by converting them into on-platform and onboard time multipliers. The coefficient value implies that the slope for the on-platform time multiplier is equal to 0.655, starting from a density of 3 passengers per square metre.

Table 2
Estimation results in Nested Logit model.

Coefficient	Name	Value (robust t-test)	Relative coefficient
$\beta^{wtt,in}$	initial waiting time	−0.165** (−4.040)	1.618
$\beta^{wtt,tb}$	waiting time when travelling backwards	−0.325** (−6.766)	3.194
$\beta^{obt,f}$	forwards onboard time	−0.102* (−4.434)	1.000 (fixed)
$\beta^{obt,b}$	backwards onboard time	−0.126** (−6.749)	1.235
β^{d}	platform passenger density	−0.655** (−5.654)	6.435
β^{l}	load factor	−0.964** (−6.159)	9.478
μ/μ_{db}	scale parameter associated with denied boarding	0.994** (12.374)	–
μ/μ_{tb}	scale parameter associated with travelling backwards	0.574** (6.470)	–

Robust t-values in parentheses.
* Robust $p < 0.05$.
** Robust $p < 0.01$.

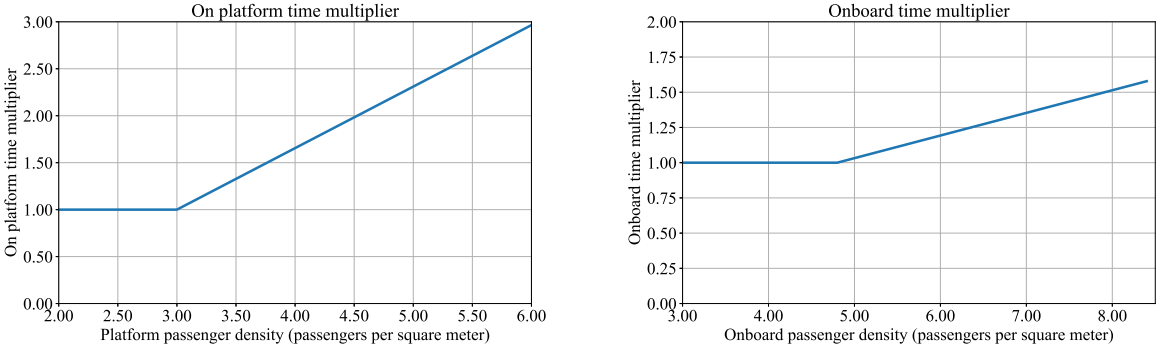

Fig. 11. On-platform time multiplier and onboard time multiplier based on passenger density.

Meanwhile, the slope for the onboard time multiplier, starting from 4.8 passengers per square metre, is set at 0.161 (= 0.964/6), since a load factor of 1 corresponds to 6 passengers per square metre in Beijing metro (Chen et al., 2016). The difference in slopes indicates that passengers are more sensitive to changes in platform density. A previous study that leveraged automated fare collection and train tracking data observed a platform pedestrian density level of approximately 1 passenger per square metre (Hänseler et al., 2020b). However, scenarios involving travelling backwards are significantly more crowded than these, suggesting that passengers' perceptions and experiences are likely to differ considerably. We consider the results reasonable for the following reasons: Waiting on the platform without boarding a metro train increases the uncertainty of arrival time, which is critical for commuters during morning rush hours. Consequently, passengers on platforms may exhibit more anxiety when facing increased density compared to when they are onboard. Furthermore, when the load factor reaches 1.0 (equivalent to an onboard density of 6 passengers per square metre), passengers perceive one minute of onboard time as 1.19 min. This perception lies between the 1.16 found by Yap et al. (2020) in the Dutch case and the 1.26 found by Hörcher et al. (2017) in the Hong Kong metro case.

Interestingly, we find that the effects of backwards onboard time are more negative, with $\beta^{obt,f} = -0.102$ and $\beta^{obt,b} = -0.126$. Compared to forwards onboard time, backwards onboard time leads to an additional 23.5% negative perception among passengers. This indicates that passengers are particularly uncomfortable with the extra onboard time associated with travelling backwards.

For waiting time, $\beta^{wtt,in}$ is estimated to be −0.165, indicating that one minute of initial waiting time is perceived as 1.618 min of forwards onboard time. This ratio is similar to the value of 1.50 found in a study from the Netherlands, which examines the ratio of perceived time outside the vehicle to time inside the vehicle (Yap et al., 2020). Other studies utilising smart card data have calibrated this ratio to 1.62 and 1.68 (Yap and Cats, 2021; Kim et al., 2020), which are slightly higher than the 1.618 observed here. These comparisons suggest that even when travelling backwards is considered, passengers' perception of initial waiting time aligns closely with existing research. However, and in contrast to our finding regarding onboard time, $\beta^{wtt,tb}$ is estimated to be −0.325, which is 1.97 times the value of $\beta^{wtt,in}$. This shows a strong aversion to waiting on the platform at turn-back stations. During backwards travel, one minute of waiting time is perceived as equivalent to 3.194 min of negative feelings while onboard. Although this perception has not been quantified in previous studies, it aligns with intuitive travel experiences, indicating that passengers find it more difficult to accept additional waiting, particularly after adopting a backwards travel strategy.

As mentioned before, the travelling backwards strategy might be adopted by passengers in cases where it can reduce passenger uncertainty on arrival time, addressing concerns about being left behind. To quantify passengers' motivations for travelling backwards, we plotted the waiting time distribution of passengers at origins and turn-back stations, as shown in Fig. 12. The average waiting time at origin stations is 643.22 s, which is significantly higher than the 251.51 s at turn-back stations. Considering the disutility factor of 1.97, the average perceived waiting time at turn-back stations can be estimated to be equivalent to 495.47 s, which is 147.75 s less than at origins. Furthermore, the average backwards onboard time is 364.22 s. With a negative utility coefficient of 0.76 (= −0.126/ − 0.165), the perceived additional onboard time is 276.81 s, which is 366.41 s less than the average waiting time

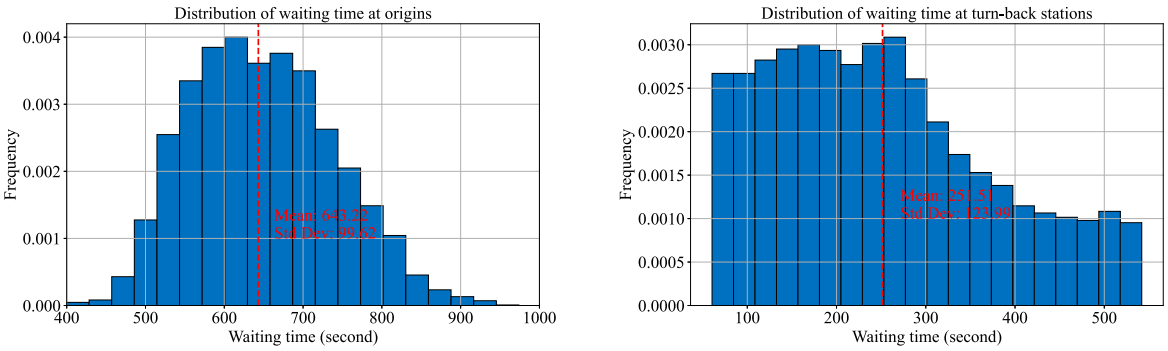

Fig. 12. Empirical distribution of waiting time at origin stations and turn-back stations.

Table 3
Estimation results with and without considering passenger transfers.

Coefficient	Without considering transfers	Relative coefficient	Considering transfers	Relative coefficient
$\beta^{wtt,in}$	−0.165** (−4.040)	1.618	−0.158** (−3.882)	1.597
$\beta^{wtt,tb}$	−0.325** (−6.766)	3.194	−0.298** (−6.627)	3.006
$\beta^{obt,f}$	−0.102* (−4.434)	1.000 (fixed)	−0.099* (−5.055)	1.000 (fixed)
$\beta^{obt,b}$	−0.126** (−6.749)	1.235	−0.110** (−7.102)	1.115
β^{d}	−0.655** (−5.654)	6.435	−0.614** (−5.056)	6.203
β^{l}	−0.964** (−6.159)	9.478	−0.938** (−6.744)	9.472
β^{n}	–	–	−0.738** (−5.525)	7.455
μ/μ_{db}	0.994** (12.374)	–	0.986** (10.769)	–
μ/μ_{tb}	0.574** (6.470)	–	0.568** (5.521)	–

Robust t-values in parentheses.
* Robust $p < 0.05$.
** Robust $p < 0.01$.

at origin stations. These factors explain why some passengers prefer the backwards travel alternative, depending on the additional waiting time at the origin station for the reverse direction and the backwards onboard time.

4.1.4. Parameter estimation results considering passenger transfers

The previous analysis was based on single-route OD pairs without considering transfers, which may not account for the effect of transfers on route choice. To extend the analysis, we applied the method proposed by Xu et al. (2019) to assign all passengers in the network to specific paths, incorporating 388,740 travel records originating from Shahe Station and Shahe Gaojiaoyuan Station for parameter calibration in the Nested Logit model. The updated utility function is given in Eq. (29), where n_i denotes the number of transfers made by passenger i, and β^n is the corresponding coefficient. Furthermore, all travel time following a transfer is included in $t_i^{obt,f}$.

$$V_i^r = \beta^{wkt} \cdot t_i^{wkt} + (\beta^{wtt,in} \cdot t_i^{wtt,in} + \beta^{wtt,tb} \cdot t_i^{wtt,tb}) \cdot (1 + \beta^d \cdot d_i) + (\beta^{obt,f} \cdot t_i^{obt,f} + \beta^{obt,b} \cdot t_i^{obt,b}) \cdot (1 + \beta^l \cdot l_i) + \beta^n \cdot n_i \quad (29)$$

When considering transfers, the Rho-square-bar value of the Nested Logit model is 0.212, and the corresponding parameter estimation results are presented in Table 3. Among these results, the relative coefficient for transfers is 7.455, which falls within the range of 5.20 and 8.48 reported in previous studies (Yap et al., 2020, 2023). This suggests that while transfers do introduce some disutility, they do not significantly intensify the negative impact of backwards travel. Additionally, the ratio of $\beta^{wtt,tb}$ to $\beta^{wtt,in}$ is 1.88, which is lower than 1.97 in the previous model. This indicates that when transfers are considered, passengers exhibit a slightly lower aversion to waiting on platforms at turn-back stations. However, the absolute difference between these two values is relatively small, revealing that the effect of transfers on passengers' time perception when travelling backwards is relatively limited. A plausible explanation is that the benefits of travelling backwards at the origin station usually do not extend to subsequent legs of a journey involving transfers. While passengers may initially travel backwards to secure a space to travel, this advantage does not endure throughout the journey, which may explain why transfers have only a marginal effect on their waiting time perception. Further analysis in Appendix B corroborates this finding, illustrating how the benefits of backwards travel diminish after the transfer station.

4.2. Model application

We analyse several policy implications from our model estimation results. Travelling backwards results from existing transport resources being unable to meet strong travel demand within a short period of time under certain service plans. Understanding travelling backwards quantitatively aids in the planning and management of PT networks. The following two case studies are

Table 4
The number of controlled passengers (Shahe station/Shahe Gaojiaoyuan station).

Ratio	7:00–7:15	7:16–7:30	7:31–7:45	7:46–8:00	8:00–8:15	8:16–8:30	8:31–8:45	8:46–9:00
5%	121/78	135/87	105/67	86/53	79/53	71/47	31/11	14/5
10%	242/156	271/174	210/133	173/107	158/107	143/93	62/22	28/10
15%	362/233	406/261	315/200	259/160	236/160	214/140	92/33	41/15
20%	483/311	541/349	420/267	345/213	315/213	285/187	123/44	55/20
25%	604/389	676/436	525/333	431/267	394/267	356/233	154/56	69/24

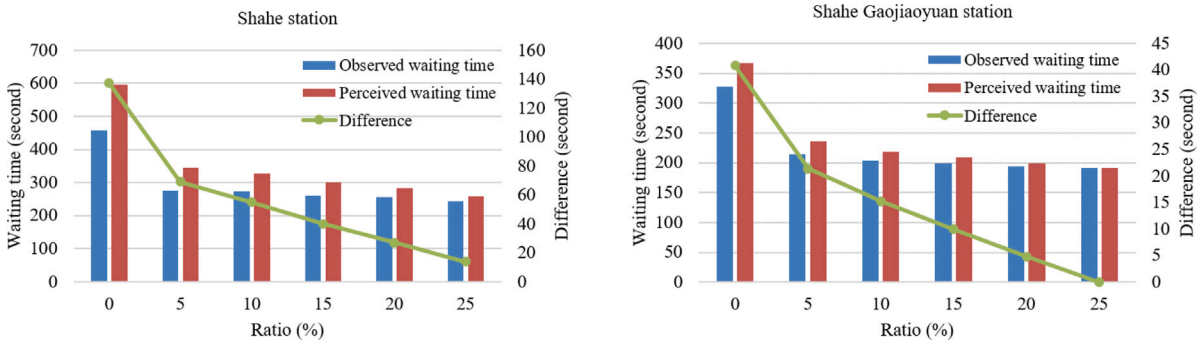

Fig. 13. Passengers' waiting time under different passenger flow control strategies.

conducted to explore these policy implications based on the passenger flow demand and transport resource supply for the Beijing metro network case study during the morning rush hours on September 26th, 2018. Please refer to Xu et al. (2019) for details of the involved passenger flow derivation method.

4.2.1. Demand management policy implication

Researchers have developed specific transport demand management strategies aimed at travelling backwards, such as passenger flow control, to alleviate the negative impact of this phenomenon (Yu et al., 2020; Shi et al., 2022). We assume that 5%, 10%, 15%, 20%, and 25% of inbound passengers are controlled from entering Shahe station and Shahe Gaojiaoyuan station every 15 min to reduce the input flow into the metro network. The number of controlled passengers is shown in Table 4. As reported in Section 3, when denied boarding occurs, 21% of passengers departing from Shahe station adopt travelling backwards, while the remaining 79% wait at the platform. For passengers departing from Shahe Gaojiaoyuan station, 9% choose the travelling backwards strategy. This experiment aims to analyse the mitigating effect of the above strategies on passengers' actual perceived waiting time.

As described in Section 4.1.3, the reduction in perceived waiting time largely drives passengers to adopt the travelling backwards strategy. We measure the average observed waiting time and perceived waiting time of passengers departing from Shahe station and Shahe Gaojiaoyuan station under different strategies, as shown in Fig. 13. As the number of controlled passengers increases, the difference between perceived waiting time and observed waiting time gradually decreases, i.e., platform passenger density decreases. When the controlled ratio reaches 25%, the corresponding difference at Shahe Gaojiaoyuan station is close to zero. This reduction further results in fewer passengers being denied boarding. Conversely, when the control ratio is small, the waiting time perceived by passengers is significantly longer than the observed waiting time. For example, with a 0% control ratio, each passenger departing from Shahe station experiences an increase of 137.23 s in perceived waiting time.

Furthermore, taking the scenario where the passenger flow control strategy is not performed (i.e., the control ratio is 0) as the baseline, we find that all the perceived saved waiting times exceed the observed saved waiting times. This means that the expected benefits of passenger flow control strategies are underestimated. For strategies with larger control ratios, the degree of underestimation is greater, especially concerning the relative saved waiting time. For example, at Shahe station, when the control ratio is 5%, the observed saved waiting time is 182.38 (458.16–275.78) seconds, while the perceived saved waiting time is 250.38 (595.39–345.01) seconds, resulting in a perceived error of 37.3%. Similarly, when the control ratio is 25%, this error reaches 57.5%. This significant error may negatively impact the calculation of expected benefits and the feasibility assessment of corresponding passenger flow control strategies.

4.2.2. Passenger behaviour guidance policy implication

Appropriate passenger behaviour guidance policies have been proven to positively impact easing congestion in metro systems (Drabicki et al., 2021). Metro operators and managers can influence passenger behaviour to some extent by providing online passenger flow information or implementing offline passenger guidance measures (Drabicki et al., 2023; Hao et al., 2024; Xu et al., 2024). In the following, we focus on the changes in perceived waiting time for each passenger when different proportions adopt the travelling backwards strategy.

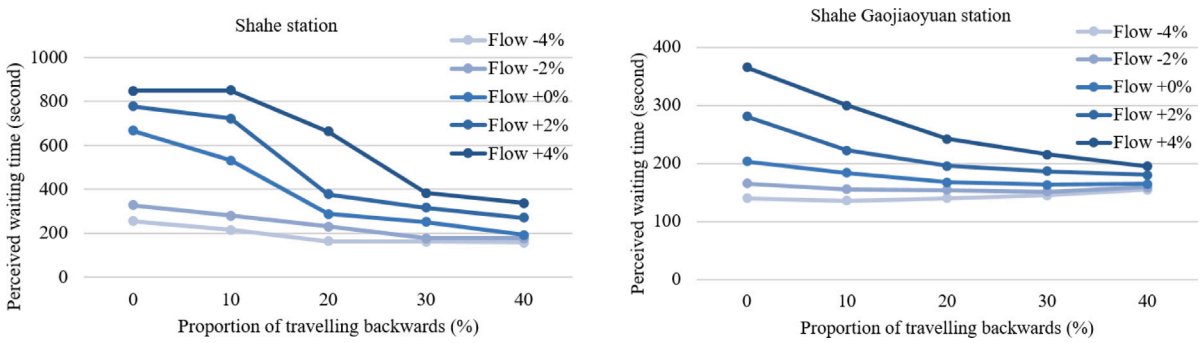

Fig. 14. Perceived waiting time under different passenger guidance strategies.

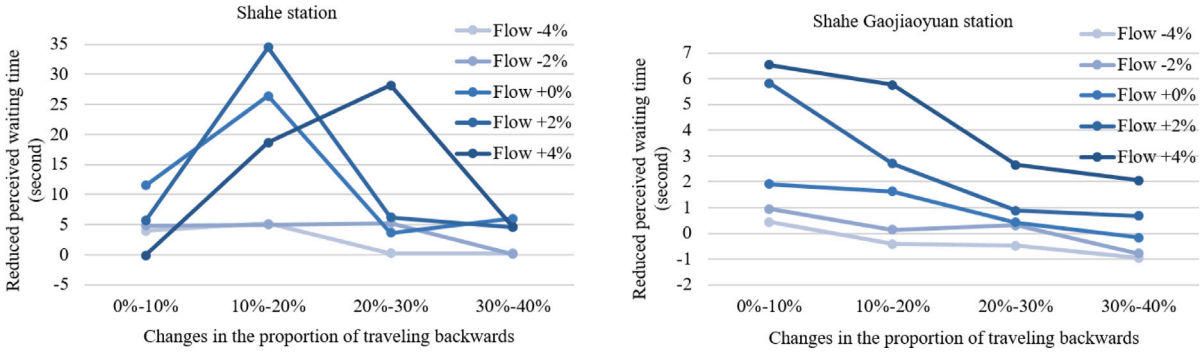

Fig. 15. Reduced perceived waiting time under different passenger guidance strategies.

In this experiment, we set the proportions of passengers adopting this strategy to 10%, 20%, 30%, and 40% when denied boarding occurs. To further investigate the most appropriate policies under different passenger flow scenarios, we conduct experiments by incrementally adjusting the original passenger flow by −4%, −2%, +0%, +2%, and +4%. We calculate the perceived waiting time of passengers departing from Shahe station and Shahe Gaojiaoyuan station, as shown in Fig. 14. The darker the curve, the greater the passenger flow is in the respective scenario.

For scenarios with smaller passenger flow (−4% and -2%), guiding more passengers to travel backwards has no effect on reducing the perceived waiting time. In fact, when the proportion of travelling backwards increases from 20% to 40%, the average perceived waiting time of each passenger increases. This is because when the passenger flow is small, waiting times at the origin are not too long. Consequently, travelling backwards does not significantly reduce waiting time and may even cause congestion at turn-back stations. Additionally, passengers' aversion to waiting at turn-back stations increases their perceived waiting time. This is consistent with expectations: when the passenger flow is low, metro operators should not guide passengers to travel backwards as it may lead to longer perceived waiting times. Conversely, for scenarios with larger passenger flow (+0%, +2%, and +4%), encouraging more passengers to adopt the travelling backwards strategy significantly reduces the overall perceived waiting time.

To quantitatively measure the potential benefit brought about by each 1% of passengers being guided to travel backwards, we calculate the reduced perceived waiting time of each passenger, as shown in Fig. 15. The x-axis of the figure depicts the change in the proportion of travelling backwards, increasing by 10%, while the y-axis shows the reduced perceived waiting time. For Shahe station, when the proportion increases from 10% to 20% under the flow +0% and +2% scenarios, the reduced perceived waiting times reach a maximum of 26.43 and 34.48 s, respectively. This means that for every 1% increase in passengers travelling backwards, the average perceived waiting time per passenger can be reduced by 26.43 s and 34.48 s. For the +4% scenario, the maximum benefit of 28.16 occurs when the proportion increases from 20% to 30%. This indicates that when passenger flow remains the same or increases by 2%, encouraging around 20% of passengers to travel backwards can bring significant benefits. However, this marginal gain decreases if we encourage more passengers to travel backwards. When passenger flow increases by 4%, this decrease in marginal returns occurs after the proportion of travelling backwards reaches 30%.

The above phenomenon can be explained by the passenger flow assignment results presented in Section 4.1.1. Adoption of the travelling backwards strategy by some passengers initially balances the distribution of load factors across trains at a macroscopic level. Higher passenger flow increases waiting times, allowing more passengers to benefit from travelling backwards. However, when a substantial number of passengers employ this strategy, congestion at the upstream station escalates, neutralising the advantages such as reduced perceived waiting times compared to those at the origin station. Thus, while the strategy initially offers significant benefits, its effectiveness diminishes as the share of passengers using it continues to rise.

For Shahe Gaojiaoyuan station, the reduced perceived waiting time in each scenario shows a downward trend as the proportion of travelling backwards increases. This suggests that encouraging around 10% of passengers to travel backwards yields significant policy benefits. The difference in policy effects between the two case study stations is attributed to the lower number of inbound passengers at Shahe Gaojiaoyuan station compared to Shahe station. Thus, in the latter case, encouraging more passengers to travel backwards is effective up to a certain point, beyond which the (accumulated) benefits diminish. Optimal guidance from the metro operators' perspective should therefore consider the current passenger flow levels to maximise the reduction in perceived waiting times without causing congestion at turn-back stations or producing other counterproductive effects.

5. Conclusion

This paper estimates a route choice model considering travelling backwards behaviour. Model estimation results contribute to our understanding of passengers' perception of time in various segments. We thereby provide new insights into passengers' perception of travel time and route choice behaviour under overcrowding situations. Choice data are constructed using smart card data and train timetable data. Furthermore, the results help better capture the real travel experience of passengers and design more targeted passenger control or guidance strategies to improve metro service levels. The estimation results show that passengers perceive backwards onboard time as 23.5% more negative than forwards onboard time. However, passengers show a much greater aversion to waiting time when travelling backwards than to their initial waiting time. Quantitatively, every minute of waiting time for passengers at the turn-back stations is equivalent to 1.97 min of waiting time at the origin platform. Despite this, the expected perceived waiting time at turn-back stations is still smaller than that at the origin, which provides an intuitive explanation for the occurrence of travelling backwards behaviour. As far as we know, this is the first study to quantify this difference in perception, providing a solid theoretical basis to assist in the formulation of relevant PT operation policies.

Several policy implications in terms of demand management and passenger behaviour guidance are explored using our estimation results. By comparing perceived waiting times under different passenger control intensities, the traditional observed waiting time indicator underestimates the expected effect of passenger control strategies. This underestimation increases with the proportion of passenger control, highlighting the need to distinguish between objective waiting time and perceived waiting time to avoid an inaccurate assessment of the implications of relevant demand management measures. Furthermore, we also test guidance policy recommendations by evaluating the expected benefits of guidance policies that encourage or inhibit travelling backwards behaviour under different passenger flow intensities. We find that guiding 20 to 30% of the passengers to travel backwards can significantly improve the passenger travel experience, depending on the overall passenger flow, with higher volumes calling for the guidance of more travellers. While passengers may not always adhere to guidance measures, the experiments conducted can still offer policy insights. For example, to encourage 20% of the passengers to adopt the travelling backwards strategy, metro operational practices can be adjusted accordingly. If more than 20% of the passengers travel backwards, implementing a skip-stop policy can help manage the excess passenger flow. In contrast, if fewer than 20% adopt this strategy, further promotion of backwards travel should be undertaken, and trains travelling in the opposite direction should not skip any stops to speed up rolling stock circulation. Similar experiments can be conducted in other overcrowded metro systems to unravel the optimal point in designing effective passenger demand control and guidance policies.

Future research can extend this study in five key areas. First, more precise revealed preference data drawn from multiple sources could deepen our understanding of travelling backwards. For instance, information on passenger occupancy in the opposite direction, or counts of passengers who remain on board at terminal stations, would allow a more detailed reconstruction of travel trajectories (Hänseler et al., 2020a). Collecting reliable information on passenger distribution through surveys or real-time video footage could also reduce errors when inferring individual crowding experiences and estimating perception-related parameters. However, such data is seldom available and is typically sparse and limited to a few locations (passages, entrances, platforms) thereby hampering the analysis undertaking in this study and greatly reducing its feasibility for large-scale or repeated applications. Second, exploring the attitudes of passengers with varying travel frequencies towards travelling backwards is an intriguing subject for future studies. We hypothesise that frequent travellers might be more inclined to adopt the travelling backwards strategy due to their familiarity with upstream station conditions. Investigating this could yield insights that aid in developing targeted policy implications, such as personalised online guidance, to enhance passenger experience and the overall level of service. Third, this study seeks to use widely available data to capture passengers' perceptions of travelling backwards, thereby guiding policy-making and practical applications. If a deeper exploration of the cognitive mechanisms underlying passenger behaviour is required, choice experiments or focus groups may be appropriate, as these methods can yield more relevant variables and permit more precise cognitive-level decision modelling. Fourth, studying additional situations related to travelling backwards is an intriguing extension of this research (Shelat et al., 2021). One such situation arises when passengers choose not to transfer at the nearest station but instead ride a few extra stops to transfer at a relatively less crowded station, ensuring a seat for the latter part of their journey. Another related scenario occurs when passengers pass a station in a non-stop train and then take another train backwards to reach their destination, for instance, on a mainline railway. Investigating passenger behaviour and travel experiences in these scenarios would contribute to a more comprehensive understanding of this unconventional route choice behaviour. Finally, incorporating the analysis of travelling backwards behaviour into infrastructure planning and service planning is essential. One of the most significant reasons for backwards travel is the imbalance in passenger demand across different rail segments. Therefore, at the planning stage, particular attention should be paid to the feasibility of train turnarounds at key locations and the availability of station yards to support such operations. Implementing targeted turnaround services in high-demand areas could help alleviate congestion and reduce the need for backwards travel, thereby improving passenger distribution and service efficiency.

CRediT authorship contribution statement

Chao Yu: Writing – original draft, Conceptualization, Methodology, Software. **Haiying Li:** Data curation, Resources. **Ziyulong Wang:** Conceptualization, Methodology, Writing – original draft. **Wei Ma:** Validation, Writing – review & editing. **Rob M.P. Goverde:** Writing – review & editing, Validation. **Oded Cats:** Writing – review & editing, Methodology, Supervision.

Appendix A. Real-life images of congestion

Despite reduced headways during peak hours, congestion remains severe in the metro system, particularly on the Changping Line in Beijing. As a result, passengers frequently adopt backwards travel as a rational strategy. Fig. A.1 illustrates congestion at: (1) Station entrances; (2) Ticket gates; (3) Station halls; (4) Train platform. In such extreme crowding conditions, many passengers opt for backwards travel to secure a spot on the train or to avoid prolonged waiting on the platform.

Fig. A.1. Real-life images of congestion on the Changping Line, Beijing.

Appendix B. Travelling backwards at different travel distances

As illustrated in Fig. B.1(1), this investigation examines nine destination stations — Gonghuacheng, Zhuxinzhuang, Shengming Kexueyuan, Xierqi, Shangdi, Wudaokou, Zhichunlu, Dazhongsi, and Xizhimen — to evaluate how journey distances influence passengers' adoption of travelling backwards tactics. Specifically, the last five destination stations — Shangdi, Wudaokou, Zhichunlu, Dazhongsi, and Xizhimen — are not located along the Changping Line. Fig. B.1(2) and (3) respectively present the proportions of backwards travellers departing from Shahe and Shahe Gaojiaoyuan stations. The analysis reveals two distinct patterns: For destinations at Xierqi station and beyond along the southward extension, the prevalence of backwards travel remains relatively consistent regardless of distance. Conversely, for northward destinations along the Changping Line proper, a clear positive correlation emerges — longer travel distances correspond to significantly higher rates of travelling backwards strategy adoption. This dichotomy demonstrates that while travelling backwards may provide immediate boarding advantages, it does not optimise passengers' post-transfer travel experience.

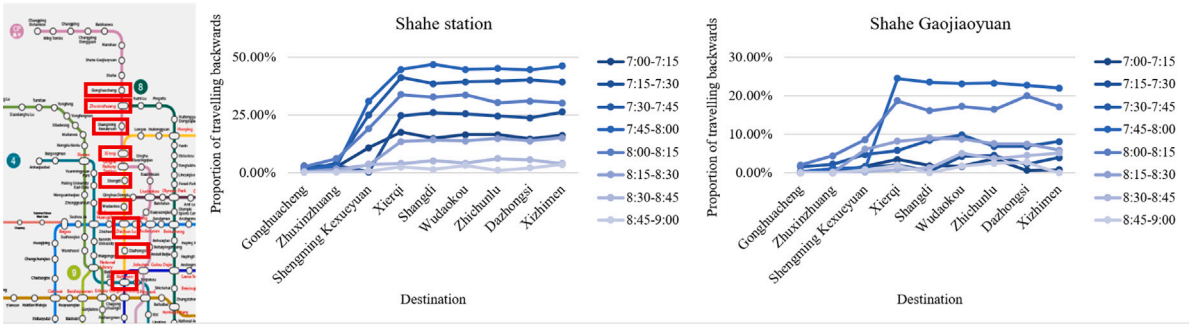

(1) Destinations (2) Proportion of passengers travelling backwards from Shahe (3) Proportion of passengers travelling backwards from Shahe Goajiaoyuan

Fig. B.1. The proportion of passengers travelling backwards at different travel distances.

References

Arbex, R., Cunha, C.B., 2020. Estimating the influence of crowding and travel time variability on accessibility to jobs in a large public transport network using smart card big data. J. Transp. Geogr. 85, 102671.

Bierlaire, M., 2016. Pythonbiogeme: A Short Introduction. Technical Report, Transport and Mobility Laboratory, EPFL, Technical Report.

Björklund, G., Swärdh, J.E., 2017. Estimating policy values for in-vehicle comfort and crowding reduction in local public transport. Transp. Res. Part A: Policy Pr. 106, 453–472.

Cats, O., West, J., Eliasson, J., 2016. A dynamic stochastic model for evaluating congestion and crowding effects in transit systems. Transp. Res. Part B: Methodol. 89, 43–57.

Chakirov, A., Erath, A., 2011. Use of public transport smart card fare payment data for travel behaviour analysis in Singapore. In: Proceedings of the 16th International Conference of Hong Kong Society for Transportation Studies. Hong Kong Society for Transportation Studies, pp. 1–11.

Chen, F., Fang, J., Wu, Q., 2016. Study of standing passenger density in subway cars based on passengers' spatial comfort: Case study of Beijing subway line 4. Transp. Res. Rec. 2540 (1), 84–91.

Drabicki, A., Cats, O., Kucharski, R., Fonzone, A., Szarata, A., 2023. Should I stay or should I board? Willingness to wait with real-time crowding information in urban public transport. Res. Transp. Bus. Manag. 47, 100963.

Drabicki, A., Kucharski, R., Cats, O., Szarata, A., 2021. Modelling the effects of real-time crowding information in urban public transport systems. Transp. A: Transp. Sci. 17 (4), 675–713.

Eltved, M., 2020. Modelling passenger behaviour in mixed schedule- and frequency-based public transport systems (Ph.D. thesis). Technical University of Denmark.

Hänseler, F.S., Van den Heuvel, J.P., Cats, O., Daamen, W., Hoogendoorn, S.P., 2020a. A passenger-pedestrian model to assess platform and train usage from automated data. Transp. Res. Part A: Policy Pr. 132, 948–968.

Hänseler, F.S., Van den Heuvel, J.P.A., Cats, O., Daamen, W., Hoogendoorn, S.P., 2020b. A passenger-pedestrian model to assess platform and train usage from automated data. Transp. Res. Part A: Policy Pr. 132, 948–968.

Hao, H., Yao, E., Chen, R., Pan, L., Wang, Y., 2024. Dynamic passenger route guidance in the multimodal transit system with graph representation and attention based deep reinforcement learning. IEEE Trans. Intell. Transp. Syst. 1–13.

Haywood, L., Koning, M., Monchambert, G., 2017. Crowding in public transport: Who cares and why? Transp. Res. Part A: Policy Pr. 100, 215–227.

Hörcher, D., Graham, D.J., Anderson, R.J., 2017. Crowding cost estimation with large scale smart card and vehicle location data. Transp. Res. Part B: Methodol. 95, 105–125.

Kim, I., Kim, H.C., Seo, D.J., Kim, J.I., 2020. Calibration of a transit route choice model using revealed population data of smartcard in a multimodal transit network. Transportation 47 (5), 2179–2202.

Kumagai, J., Wakamatsu, M., Managi, S., 2021. Do commuters adapt to in-vehicle crowding on trains? Transportation 48, 2357–2399.

Li, Y., Zhou, F., Hong, L., Zhu, W., 2017. Empirical analysis of failing to board and traveling backward in an overcrowded urban rail transit system. In: 17th COTA International Conference of Transportation Professionals. American Society of Civil Engineers Reston, VA, pp. 1979–1989.

Ma, W., Qian, Z.S., 2017. On the variance of recurrent traffic flow for statistical traffic assignment. Transp. Res. Part C: Emerg. Technol. 81, 57–82.

Myung, I.J., 2003. Tutorial on maximum likelihood estimation. J. Math. Psych. 47 (1), 90–100.

Nelson, H.E., 2002. Emergency movement. SFPE Handb. Fire Prot. Eng.

Othman, N.B., Legara, E.F., Selvam, V., Monterola, C., 2015. A data-driven agent-based model of congestion and scaling dynamics of rapid transit systems. J. Comput. Sci. 10, 338–350.

Pel, A.J., Bel, N.H., Pieters, M., 2014. Including passengers' response to crowding in the Dutch national train passenger assignment model. Transp. Res. Part A: Policy Pr. 66, 111–126.

Raveau, S., Guo, Z., Muñoz, J.C., Wilson, N.H.M., 2014. A behavioural comparison of route choice on metro networks: Time, transfers, crowding, topology and socio-demographics. Transp. Res. Part A: Policy Pr. 66, 185–195.

Raveau, S., Muñoz, J.C., De Grange, L., 2011. A topological route choice model for metro. Transp. Res. Part A: Policy Pr. 45 (2), 138–147.

Schneider, A., Krueger, E., Vollenwyder, B., Thurau, J., Elfering, A., 2021. Understanding the relations between crowd density, safety perception and risk-taking behavior on train station platforms: A case study from Switzerland. Transp. Res. Interdiscip. Perspect. 10, 100390.

Shelat, S., Cats, O., Van Lint, J., 2021. Quantifying travellers' evaluation of waiting time uncertainty in public transport networks. Travel. Behav. Soc. 25, 209–222.

Shi, J., Qin, T., Yang, L., Xiao, X., Guo, J., Shen, Y., Zhou, H., 2022. Flexible train capacity allocation for an overcrowded metro line: A new passenger flow control approach. Transp. Res. Part C: Emerg. Technol. 140, 103676.

Tirachini, A., Hurtubia, R., Dekker, T., Daziano, R.A., 2017. Estimation of crowding discomfort in public transport: Results from Santiago de Chile. Transp. Res. Part A: Policy Pr. 103, 311–326.

Tirachini, A., Sun, L., Erath, A., Chakirov, A., 2016. Valuation of sitting and standing in metro trains using revealed preferences. Transp. Policy 47, 94–104.

Xu, X., Li, H., Liu, J., Ran, B., Qin, L., 2019. Passenger flow control with multi-station coordination in subway networks: algorithm development and real-world case study. Transp. B: Transp. Dyn. 7 (1), 446–472.

Xu, R., Li, Y., Zhu, W., Li, S., 2018. Empirical analysis of traveling backwards and passenger flows reassignment on a metro network with automatic fare collection (AFC) data and train diagram. Transp. Res. Rec. 2672 (8), 230–242.

Xu, X., Liu, J., Zhang, A., Xielan, S., Li, Z., Liu, J., Ran, B., 2024. The impacts of COVID-19 on route choice with guidance information in urban rail transit of megacities. Transp. Res. Part A: Policy Pr. 183, 104046.

Yap, M., Cats, O., 2021. Taking the path less travelled: Valuation of denied boarding in crowded public transport systems. Transp. Res. Part A: Policy Pr. 147, 1–13.

Yap, M., Cats, O., Van Arem, B., 2020. Crowding valuation in urban tram and bus transportation based on smart card data. Transp. A: Transp. Sci. 16 (1), 23–42.

Yap, M., Wong, H., Cats, O., 2023. Public transport crowding valuation in a post-pandemic era. Transportation 1–20.

Yu, C., Li, H., Xu, X., Liu, J., 2020. Data-driven approach for solving the route choice problem with traveling backward behavior in congested metro systems. Transp. Res. Part E: Logist. Transp. Rev. 142, 102037.

Zhao, J., Zhang, F., Tu, L., Xu, C., Shen, D., Tian, C., Li, X.Y., Li, Z., 2016. Estimation of passenger route choice pattern using smart card data for complex metro systems. IEEE Trans. Intell. Transp. Syst. 18 (4), 790–801.

Zhou, Y., Chen, J., Zhong, M., Li, Z., Zhou, W., Zhou, Z., 2023. Risk analysis of crowd gathering on metro platforms during large passenger flow. Tunn. Undergr. Space Technol. 142, 105421.

Zhu, Y., Koutsopoulos, H.N., Wilson, N.H.M., 2017. A probabilistic Passenger-to-Train Assignment Model based on automated data. Transp. Res. Part B: Methodol. 104, 522–542.

Zhu, Y., Koutsopoulos, H.N., Wilson, N.H., 2018. Inferring left behind passengers in congested metro systems from automated data. Transp. Res. Part C: Emerg. Technol. 94, 323–337.